This Accepted Manuscript has not been copyedited and formatted. The final version may differ from this version.

JNeurosci
THE JOURNAL OF NEUROSCIENCE

Research Articles: Behavioral/Cognitive

Dreaming in NREM sleep: a high-density EEG study of slow waves and spindles

Francesca Siclari[1], Giulio Bernardi[1,3], Jacinthe Cataldi[1] and Giulio Tononi[2]

[1]*Lausanne University Hospital and University of Lausanne, Switzerland*
[2]*Dpt of Psychiatry, University of Wisconsin-Madison, WI, USA*
[3]*MoMiLab Unit, IMT School for Advanced Studies Lucca, Lucca, Italy*

DOI: 10.1523/JNEUROSCI.0855-18.2018

Received: 29 March 2018

Revised: 30 July 2018

Accepted: 1 August 2018

Published: 10 September 2018

Author contributions: F.S. and G.T. designed research; F.S. and J.C. performed research; F.S. and G.B. analyzed data; F.S. wrote the first draft of the paper; F.S., G.B., and G.T. edited the paper; F.S. wrote the paper.

Conflict of Interest: The authors declare no competing financial interests.

This work was supported by the Swiss National Science Foundation Grants PZ00P3_173955 (F.S.), the Divesa Foundation Switzerland (F.S.), the Pierre-Mercier Foundation for Science (F.S.), the Bourse Pro-Femme of the University of Lausanne (F.S.), and an EMBO short-term postdoctoral fellowship (G.B.), the NIH/NCCAM P01AT004952 (G.T.), NIH/NIMH 5P20MH077967 (G.T.), the Tiny Blue Dot Inc. MSN196438/AAC1335 (G.T.).

Corresponding author: Francesca Siclari, Center for Research and Investigation in Sleep (CIRS), Lausanne University Hospital (CHUV), Rue du Bugnon 46, 1011 Lausanne, Switzerland., francesca.siclari@chuv.ch

Cite as: J. Neurosci ; 10.1523/JNEUROSCI.0855-18.2018

Alerts: Sign up at www.jneurosci.org/cgi/alerts to receive customized email alerts when the fully formatted version of this article is published.

Accepted manuscripts are peer-reviewed but have not been through the copyediting, formatting, or proofreading process.

Copyright © 2018 the authors

JNeurosci Accepted Manuscript

JNeurosci Accepted Manuscript

Dreaming in NREM sleep:
a high-density EEG study of slow waves and spindles

Francesca Siclari[1], Giulio Bernardi[1,3], Jacinthe Cataldi[1], Giulio Tononi[2]

[1] *Lausanne University Hospital and University of Lausanne, Switzerland*
[2] *Dpt of Psychiatry, University of Wisconsin-Madison, WI, USA*
[3] *MoMiLab Unit, IMT School for Advanced Studies Lucca, Lucca, Italy*

Corresponding author:

Francesca Siclari
Center for Research and Investigation in Sleep (CIRS)
Lausanne University Hospital (CHUV)
Rue du Bugnon 46
1011 Lausanne, Switzerland.
francesca.siclari@chuv.ch

Abbreviated title: dreaming in NREM sleep
11 Figures
Word count: Abstract 186 words, Introduction 718 words, Discussion 1593 words

The authors do not have any conflict of interest to declare.

Acknowledgements: This work was supported by the Swiss National Science Foundation Grants PZ00P3_173955 (F.S.), the Divesa Foundation Switzerland (F.S.), the Pierre-Mercier Foundation for Science (F.S.), the Bourse Pro-Femme of the University of Lausanne (F.S.), and an EMBO short-term postdoctoral fellowship (G.B.), the NIH/NCCAM P01AT004952 (G.T.), NIH/NIMH 5P20MH077967 (G.T.), the Tiny Blue Dot Inc. MSN196438/AAC1335 (G.T.).

JNeurosci Accepted Manuscript

Abstract

Dreaming can occur in both rapid eye movement (REM) and Non-REM (NREM) sleep. We recently showed that in both REM and NREM sleep, dreaming is associated with local decreases in slow wave activity (SWA) in posterior brain regions. To expand these findings, here we asked how specific features of slow waves and spindles, the hallmarks of NREM sleep, relate to dream experiences. Fourteen healthy human subjects (10 females) underwent nocturnal high-density EEG recordings combined with a serial awakening paradigm. Reports of dreaming, compared to reports of no experience, were preceded by fewer, smaller and shallower slow waves, and faster spindles, especially in central and posterior cortical areas. We also identified a minority of very steep and large slow waves in frontal regions, which occurred on a background of reduced SWA and were associated with high-frequency power increases (local 'micro-arousals') heralding successful recall of dream content. These results suggest that the capacity of the brain to generate experiences during sleep is reduced in the presence of neuronal off-states in posterior and central brain regions, and that dream recall may be facilitated by the intermittent activation of arousal systems during NREM sleep.

Significance statement

By combining high-density EEG recordings with a serial awakening paradigm in healthy subjects, we show that dreaming in NREM sleep occurs when slow waves in central and posterior regions are sparse, small and shallow. We also identified a small subset of very large and steep frontal slow waves that are associated with high-frequency activity increases (local 'micro-arousals') heralding successful recall of dream content. These results provide noninvasive measures that could represent a useful tool to infer the state of consciousness during sleep.

JNeurosci Accepted Manuscript

Introduction

What determines the level of consciousness during sleep? Why are we sometimes unconscious, while at other times we have vivid conscious experiences in the form of dreams? When rapid eye movement (REM) sleep was first described in humans (Aserinsky and Kleitman, 1955), the explanation seemed relatively straightforward: 74% of subjects woken up during this state reported that they had been dreaming, compared to only 17% awakened at other times. It is not surprising that following this observation, Aserinsky and Kleitman claimed to have 'furnished the means of determining the incidence and duration of periods of dreaming' (Aserinsky and Kleitman, 1955). Indeed, the fast-frequency, desynchronized EEG activity of REM sleep, similar to the waking EEG, appeared to offer the ideal premises for conscious experiences to occur. In the following years, however, the assumption that dreaming and conscious experiences were synonymous with REM sleep was challenged (Solms, 2000). Pharmacological suppression of REM sleep, for instance, did not eliminate dreaming (Oudiette et al., 2012), and specific forebrain lesions (Solms, 2000) were shown to suppress dreaming without affecting REM sleep. In addition, by changing the question from 'Tell me whether you had a dream' to 'Tell me what was going through your mind', reports of conscious experiences in Non-REM (NREM) sleep were obtained in up to 70 % of cases (Stickgold et al., 2001). Especially in the early morning hours, NREM sleep dream reports appeared indistinguishable from REM sleep dream reports (Monroe et al., 1965; Antrobus et al., 1995). This raised the question of whether slow waves, which decrease across the night as a function of homeostatic sleep pressure, may interfere with the generation of dream experiences. Experimental and theoretical work offers plausible explanations of why this should be so: neuronal off-periods associated with slow waves disrupt causal interactions between thalamo-cortical regions (Massimini et al., 2005; Pigorini et al., 2015), thereby impairing information integration, which has been proposed as a prerequisite for

JNeurosci Accepted Manuscript

consciousness (Tononi, 2008). Initial attempts to relate EEG changes in slow wave activity (SWA, 1-4 Hz spectral power) to dreaming yielded variable results (Williamson et al., 1986; Esposito et al., 2004; Chellappa et al., 2011; Marzano et al., 2011). In recent years, it has become clear that the alternation between off- and on-periods underlying the surface EEG slow wave is not global, but occurs mostly locally, meaning that it can occur out-of-phase with respect to other cortical regions (Nir et al., 2011). It has also become clear that conventional EEG recordings comprising only a few electrodes would not be able to capture such local SWA changes. Besides, slow waves with neuronal off-periods have been shown to occur not only in NREM sleep, but also in superficial cortical layers of primary sensory cortices in REM sleep in mice (Funk et al., 2016). To account for these aspects, in a recent study we used high-density EEG to investigate changes in brain activity associated with dreaming. We demonstrated that reports of dreaming were preceded by decreases in SWA in both REM and NREM sleep. These decreases were not global, but spatially restricted to a 'posterior hot zone' of the brain, suggesting that local changes in SWA may account for the presence of dreaming or unconsciousness *across* different behavioral states. Here we aimed to extend these findings. Instead of assessing spectral power, a rough estimate of both slow wave number and amplitude, we investigated how specific characteristics of slow waves relate to dreaming. Indeed, specific slow waves features have been shown to reflect different aspects of neuronal oscillations (Esser et al., 2007; Riedner et al., 2007; Vyazovskiy et al., 2007), including the degree of cortical bistability (density), the number of neurons that simultaneously enter a down-state (amplitude), and synaptic strength (slope). Based on these criteria, we were recently able to characterize two types of slow waves (Siclari et al., 2014; Bernardi et al.): widespread, steep and large-amplitude type I slow waves in fronto-central brain regions that are likely generated by a subcortico-cortical synchronization process, and type II slow waves with a smaller amplitude and slope and a more variable regional involvement,

JNeurosci Accepted Manuscript

which are likely generated by a cortico-cortical synchronization process. To determine how these two types of slow waves relate to dreaming, and to extend our findings to sleep spindles, we analyzed high-density-EEG recordings of 14 healthy participants who underwent a serial awakening paradigm.

Materials and methods

Participants and procedure

Fourteen healthy participants (age 33.6 ± 8.5 yrs (mean ± SD), range 22-47 yrs, 10 females) screened for medical, neurological and psychiatric disorders participated in the study. None of the subjects was on psychotropic medication. All the participants had a good sleep quality as assessed by the Pittsburgh Sleep Quality Index (< 5 points) and scored within normal limits on the Epworth Sleepiness Scale. Dream characteristics and spectral power changes associated with dreaming in the delta (1-4 Hz) and gamma frequency ranges (20-50 Hz) of subjects 1 to 7, but not slow wave nor spindle findings, have been previously reported (experiment 2, (Siclari et al., 2017)), while subjects 8-14 were newly included. Subjects 1 to 7 were acquired at the University of Wisconsin-Madison, while subjects 8-14 were studied at the Lausanne University Hospital. Written informed consent was obtained from each participant and the study was approved as part of a larger project by the local ethical committees (University of Wisconsin Madison and Lausanne University Hospital). Participants were recorded with hd-EEG (256 electrodes) while they slept in the sleep laboratory. Throughout the night, they were awakened repeatedly (Siclari et al., 2013) and asked to report whether, just before the awakening, they had been experiencing anything (dream experience, DE), had been experiencing something but could not remember the

JNeurosci Accepted Manuscript

content (dream experience without recall of content, DEWR) or had not been experiencing anything (no experience, NE) (Siclari et al., 2013). The serial awakening protocol has previously been reported in detail (Siclari et al., 2013). Awakenings were performed using a computerized alarm sound lasting 1.5s.

All subjects were studied by the first author of this paper and underwent the same serial awakening paradigm (Siclari et al., 2013), except for the fact that Madison subjects were studied for 5-10 nights while Lausanne subjects underwent only 2 study nights. As a consequence, Madison subjects had more total awakenings compared to Lausanne subjects (113.6 ± 26.0 vs 24.86 ± 8.23 per subject, $p<0.001$, unpaired two-tailed t-tests). No differences between the two groups were observed in the proportion of NREM sleep awakenings with respect to total awakenings (75.00 ± 5.30 % vs 78.81 ± 2.60%), in the proportion of N2 or N3 awakenings with respect to NREM (N2 + N3) awakenings (55.9 ± 13.69% vs 53.45 ± 22.71% N2 awakenings, $p=0.81$), and in the proportion of DE (30.96 ± 14.49 % vs 34.13 ± 20.64 %, $p=0.74$), DEWR (38.55 ± 13.88 vs 40.30 ± 21.40, $p=0.86$) and NE (30.50 ± 21.75 vs 24.97 ± 24.69, $p=0.66$) in NREM sleep. The study groups did not differ significantly in terms of age (31.57 ± 8.5 vs 35.71 ± 8.6, $p=0.38$) and female/male distribution (4/7 vs 5/7 females, $p=0.57$, Pearson's Chi-Square). All the comparisons reported herein were performed within subjects.

Recordings

Sleep recordings were carried out using a 256-channel high-density EEG (hd-EEG) system (Electrical Geodesics, Inc., Eugene, Ore.). Four of the 256 electrodes placed at the outer canthi of the eyes were used to monitor eye movements and submental electromyography was recorded

JNeurosci Accepted Manuscript

using the Electrical Geodesics polygraph input box. The EEG signal was sampled at 500 Hz and off-line band-pass filtered between 0.3 and 50 Hz for the first set of participants (subjects 1-7), and between 0.3 and 45 Hz for the second set of participants (subject 8-14, because of the different frequencies of electrical artifacts in the US and Europe). All the analyses were performed on frequency bands available for both studies (below 40 Hz). Sleep scoring was performed over 30s epochs according to standard criteria (Iber et al., 2007).

Preprocessing of data

The signal corresponding to the 2 mins preceding each awakening in stages N2 and N3 was extracted and considered for analysis. Channels containing artifactual activity were visually identified and replaced with data interpolated from nearby channels using spherical splines (NetStation, Electrical Geodesic Inc.). To remove ocular, muscular, and electrocardiograph artifacts we performed Independent Component Analysis (ICA) using EEGLAB routines (Delorme and Makeig, 2004). Only ICA components with specific activity patterns and component maps characteristic of artifactual activity were removed (Jung et al., 2000).

Slow wave detection

For slow wave detection, we used an automatic detection algorithm that was adapted from a previous study (Siclari et al., 2014). The EEG signal was referenced to the average of the two mastoid electrodes, downsampled to 128 Hz and band-pass-filtered (0.5-4 Hz, stop-band at 0.1 and 10 Hz) using a Chebyshev Type II filter (Matlab, The Math Works Inc, Natick, MA). Only slow waves with a duration between 0.25 and 1s were considered. The algorithm was applied to all channels and the following slow wave parameters were analyzed: density, negative peak amplitude, slope 1 (between the first zero crossing and the negative peak), slope 2 (between the

JNeurosci Accepted Manuscript

179 negative peak and the second zero crossing) and number of negative peaks. For an initial,
180 explorative analysis, we considered large amplitude slow waves separately from other slow
181 waves. Large amplitude slow waves (>75th percentile) were identified for each subject separately,
182 by determining the amplitude corresponding to the 75th percentile of the amplitude distribution of
183 all slow waves (all the 2-minute segments preceding awakenings in in N2 and N3 were
184 concatenated for this analysis).
185
186 *Separation between type I and type II slow waves*
187 Then, for a more precise separation between type I and type II slow waves, we used a previously
188 described approach (Bernardi et al.), which also has the advantage that it can classify slow waves
189 independently of their topographical distribution. We first created a single timing reference. To
190 do this, the negative signal envelope was generated by selecting the fifth most negative sample
191 across all mastoid-referenced channels for each time point. The fifth most negative channel was
192 arbitrarily selected instead of the most negative channel to avoid including residual high-
193 amplitude artifacts (Siclari et al., 2014; Bernardi et al., 2016). Then, a slow wave detection
194 procedure was applied to this composite signal after band-pass filtering (0.5-40 Hz). To
195 distinguish between type I and type II slow waves, for each detection we calculated a
196 synchronization score defined as the scalp involvement (-expressed as the percentage of channels
197 showing a negative averaged current value < -5 μV in the 40ms time-window centered on the
198 wave peak) multiplied by the mean slope of the slow wave (i.e., the mean of slope-1 and slope-2)
199 (Bernardi et al.). The 5μV criterion is an arbitrary cutoff to exclude small baseline fluctuations
200 that are likely unrelated to slow waves (Siclari et al., 2014; Bernardi et al., 2016). Based on the
201 distribution of the synchronization scores of all the slow waves in N2 and N3, we defined an
202 absolute threshold that corresponded to 4 median absolute deviations (MAD) from the median.

JNeurosci Accepted Manuscript

This threshold was calculated for each subject separately. Type I slow waves were defined as slow waves characterized by a synchronization score greater than the threshold, while remaining slow waves were classified as type II.

Spectral power analysis

To calculate spectral power changes associated with type I and type II slow waves, we computed power spectral density (PSD) for each channel in two 6-second periods: a pre-wave period (ending 1s before the first zero-crossing of the slow wave detected in the composite reference signal) and a post-wave period (starting 1s after the second zero-crossing of the slow wave). Spectral power was calculated in 2s Hamming windows using the Welch's modified periodogram method (implemented with the *pwelch* function in Matlab). We then averaged pre- and postwave spectral power across the three 2s bins for each channel. To evaluate changes in spectral power induced by type I and type II slow waves, we subtracted post-wave power from the pre-wave power and expressed changes as %, so that positive values represent increases in post-wave with respect to pre-wave power, while negative values represent decreases in post-wave with respect to pre-wave power. All the analyses were performed within subjects first, then averaged across subjects.

Source modeling

In order to evaluate the cortical localization of high-frequency power increases after type I slow waves, a source modelling analysis of the 18-30 Hz band-pass filtered signal was performed using GeoSource 3.0 (NetStation, Electrical Geodesics, Inc). A four-shell head model based on the Montreal Neurological Institute (MNI) atlas and standard electrode coordinates were used to

JNeurosci Accepted Manuscript

construct the forward model. The inverse matrix was defined using the standardized low-resolution brain electromagnetic tomography (sLORETA) method (Tikhonov regularization, $\lambda = 10^{-2}$). The source modelling analysis was performed on 6s windows preceding and following type I slow waves, and RMS values in the specified frequency range were used to compute relative post-pre variations. These values were averaged across slow waves and subjects.

Spindle detection

Spindle detection was based on an automatic algorithm, adapted from a previous study (Ferrarelli et al., 2007). The average-referenced signal was downsampled to 128 Hz and band-pass filtered between 11 and 16 Hz (-3 dB at 10 and 17 Hz). The following spindle parameters were analyzed: density, maximal amplitude, and frequency. Based on a previous studies (Anderer et al., 2001; Andrillon et al., 2011; Molle et al., 2011), we categorized spindles as fast or slow based on an individualized threshold, which was defined as the intermediate value between the average spindle frequency in one centroparietal (Pz) and one frontal (Fz) channel (Siclari et al., 2014).

Experimental Design and Statistical Analysis

Statistical analyses were carried out in Matlab (MathWorks Inc., Natick, MA). Analyses regarding general slow wave properties (those presented in Fig. 7, 8C, 8D and 8E), were carried out on the totality of the available signal (120s before the awakening), while analyses referring to dream reports (i.e., comparisons between DE, NE and DEWR shown in Fig. 1, 2, 3, 4, 5, 6, 8B, 10 and 11) were performed on slow wave and spindle parameters in the 60s before the awakening. Topographical analyses were limited to the 185 most inner channels to avoid the common artifactual contamination of electrodes located on the cheeks and neck.

JNeurosci Accepted Manuscript

To compare brain activity between DE and NE (and DEWR, when applicable), slow wave and spindle parameters were first averaged within the 60 seconds preceding each awakening for each subject. We then averaged the slow wave and spindle parameters associated with DEs and NEs within each subject. Whole-brain group-level comparison on average slow wave and spindle were performed using a cluster-based correction for multiple comparisons (Nichols and Holmes, 2002). Two-tailed paired t-tests with a corrected $p < 0.05$ threshold were performed. The number of subjects for each comparison is indicated in the figure legends. Correction for multiple comparisons was ensured using a permutation-based supra-threshold cluster analysis (Nichols and Holmes, 2002; Huber et al., 2004). In brief, for each comparison new datasets were generated by randomly relabeling the condition label from original data and paired t-tests were performed (N=5000). For each iteration, the maximal size of the resulting significant clusters of electrodes was stored to generate a cluster size distribution. Then, the 95th percentile of this distribution was used as the critical cluster-size threshold, to achieve cluster-corrected p-values corresponding to $\alpha < 0.05$. We did not perform an additional correction for multiple comparisons based on the number of contrasts for slow wave and spindle parameters because many of these are not truly independent, but highly correlated.

To investigate the correlation between slow wave amplitude in frontal and occipital regions (Fig. 7), we first averaged, for each 2-min data segment, slow wave amplitude within two regions of interest: Fz and Oz and immediately adjacent electrodes. We then correlated these frontal and occipital values within subjects, by taking account all the NREM segments (Spearman rank correlation). Statistical significance was determined using a permutation-based approach. Specifically, null distributions with properties that are comparable to those of the original (real)

JNeurosci Accepted Manuscript

distributions were generated by randomly shuffling the two variables of interest (frontal and occipital amplitude of slow waves) in each subject (using all available data segments) and recalculating the group-level mean correlation (n = 1,000). This null-distribution was then used to calculate the significance level of real group-level correlation values ($p < 0.05$). The same procedure was performed to test the correlation between the amplitude of large frontal slow waves (>75th percentile) and occipital slow waves (without an amplitude threshold).

For the correlation between the synchronization index of type I and type II slow waves and preceding SWA (Fig. 8C), we extracted, for each channel, the power spectral density in the 6s-window preceding each type I and type II slow wave detected in the reference signal. We then correlated spectral power and the synchronization index for each subject and channel using a Spearman rank correlation. Statistical significance was determined using the same permutation-based approach described above.

Results

Of the 969 awakenings performed across all subjects, 735 were performed in NREM sleep stages N2 and N3. Of these, 246 (33.5%) yielded reports of DE, 284 (38.6%) of DEWR and 204 (27.8%) of NE. Two subjects did not present NE in NREM sleep.

Slow waves and dreaming

Slow waves preceding reports of DE, as compared to NE, were significantly less numerous, had a smaller amplitude and slope (*corrected* p < 0.05) and displayed a trend towards more negative

JNeurosci Accepted Manuscript

peaks (*uncorrected* $p < 0.05$). These differences were relatively widespread, but the strongest statistical effects were observed in posterior and central brain regions (Fig. 1, see also Fig. 2 for mean absolute values, mean differences and uncorrected statistics). Similar results for amplitude and slope were obtained when comparing DEWR and NE (Fig. 3), while the contrast between DE and DEWR did not yield any significant differences (*not shown*), suggesting these findings reflect differences in dreaming, and not in the ability to recall the content of the dream.

Next, based on our previous work, in which we identified two types of slow waves that differ in amplitude, we performed an explorative analysis focusing exclusively on high-amplitude slow waves, using an arbitrary minimal threshold corresponding to the 75th percentile of the negative peak. This threshold was calculated for each channel and subject separately, by considering all the detected slow waves in NREM sleep. Consistent with the previous analysis (Fig. 1), reports of DE were preceded by fewer high-amplitude slow waves compared to NE, particularly in central and posterior brain areas (Fig. 4). However, DE were also associated with significantly larger and steeper high-amplitude slow waves in frontal regions (*corrected* $p < 0.05$, Fig. 4, see also Fig. 5 for mean absolute values, mean differences and uncorrected statistics), which displayed a trend towards fewer negative peaks (*uncorrected* $p < 0.05$). An additional analysis (Fig. 6) revealed that frontal high-amplitude slow waves were even larger and steeper when the content of the dream could be recalled (DE), as opposed when to when subjects reported dreaming but could not remember the content (DEWR), while no significant differences were found between DEWR and NE (*not shown*).

Taken together, these results suggest that dream experiences are more likely to occur when slow waves are sparse, small and shallow, particularly in posterior and central brain regions. In addition, by applying a minimal amplitude threshold, we identified a small minority of very

JNeurosci Accepted Manuscript

steep, high-amplitude slow waves in anterior cortical regions that tend to precede reports of dream experiences with recall of content.

Since we showed that dreaming tends to occur when slow wave amplitude in posterior regions is low (Fig. 1), we asked whether the frontal high-amplitude slow waves were associated with reductions in slow wave amplitude in posterior areas. To this aim, we first tested the correlation between the amplitude of slow waves (without an amplitude threshold) detected in a frontal region (Fz and immediately neighboring electrodes) and an occipital region of interest (Oz and immediately neighboring electrodes) for all 2min-NREM segments in each subject. This analysis revealed, as expected, a strong positive correlation between the amplitude of frontal and occipital slow waves (Spearman rank correlation coefficient $R = 0.86$, $p<0.001$), meaning that all waves considered, NREM segments with large frontal slow waves also tend to contain large occipital slow waves. Next, we correlated the amplitude of the large slow waves (above the 75^{th} amplitude percentile) in the frontal region of interest with the amplitude of slow waves in the occipital region of interest (without an amplitude threshold). Here a significant negative correlation emerged (Spearman rank correlation coefficient $R= -0.19$, $p=0.002$). It therefore appears that the larger the subset of high-amplitude slow waves in the frontal cortex, the smaller the slow waves in the occipital cortex.

These results suggest that there are two distinct populations of slow waves that differentially relate to dream reports and whose amplitudes are anti-correlated (Fig. 7). In order to achieve a more accurate and topography-independent classification of the two types of slow waves, for further analyses we used a previously described approach, (Bernardi et al.) that divides slow waves into putative type I slow waves (minority of large and steep slow waves with fronto-

JNeurosci Accepted Manuscript

central involvement) and type II slow waves (majority of smaller, shallower, diffusely distributed slow waves) based on a synchronization index taking into account their amplitude and slope (see Methods section for details). This method is based on a single temporal reference representing all sources ('negative-envelope' of the signal), and can thus classify slow waves regardless of their origin and scalp distribution. Because these analysis are mainly aimed at investigating how distinctive properties of type I slow waves relate to dream experiences, a stringent arbitrary threshold was applied in order to separate type I from potentially large type II slow waves. More specifically, only slow waves with a synchronization index greater than 4 standard median absolute deviations (MAD) from the median of all slow waves were considered type I slow waves, while the remainder of slow waves were considered type II slow waves. The large majority of slow waves classified as type I according to this method (95.0 ± 4.5 %, mean across all channels) had an amplitude above the 75th percentile; i.e., were classified as 'large' based on the amplitude criterion used in previously described analyses (Fig. 8A). In contrast, only about half of type II slow waves (52.6 ± 4.1 %) had a large amplitude.

We then computed the ratio between type I and type II slow waves for each NREM period preceding awakenings, and found that it was significantly different between DE, DEWR and NE (one-way repeated measure ANOVA, $F_{(2,12)}$=5.795, p=0.008), with DE (0.10 ± 0.01) having a significantly higher ratio compared to DEWR (0.05 ±0.01, p= 0.04, paired two-tailed t-test) and NE (0.04 ±0.01, p= 0.02), while the latter two categories did not differ significantly (p=0.4) (Fig 8B).

Next, we explored the direction of the negative association we observed between the amplitude of large frontal slow waves and occipital slow waves (Fig. 7). More specifically, we wanted to know

JNeurosci Accepted Manuscript

371 whether type I slow waves were more likely to occur on an EEG background of small slow waves
372 or whether they induced reductions of slow wave amplitude, particularly in posterior areas. To
373 this aim we first examined the correlation between SWA in the six seconds preceding each slow
374 wave and the synchronization index of that slow wave. This analysis revealed that type I slow
375 waves were more likely to be large and steep (i.e., to have a higher synchronization index) if they
376 occurred on a background of low SWA, while for type II slow waves the opposite effect was true
377 (Fig. 8C). We then examined changes in spectral power induced by type I and type II slow waves
378 (in the six seconds following the slow wave). We found that on average, type I slow waves
379 induced increases in spectral power in all frequency bands, with a small peak in the 10-12 Hz
380 range and a larger peak in the 18-30 Hz range (Fig. 8D). A source modeling analysis revealed
381 that the 18-30 Hz increases following type I slow waves peaked in fronto-central regions
382 including the medial primary motor cortex and the mid-cingulate cortex (top 5% of voxels, Fig.
383 8E). EEG examples of high frequency increases following type I slow waves are shown in Fig. 9.
384 For type II slow waves, these changes were less pronounced, and peaked in the fast spindle range
385 (around 13-14 Hz). Type I slow waves induced significantly larger power increases in the 0-2 Hz
386 and 18-40 Hz frequency ranges compared to type II slow waves (Fig. 8D). Importantly, overall,
387 neither type I nor type II slow waves induced decreases in SWA. These results show that type I
388 slow waves tend to occur when SWA is low, but do not appear to consistently induce reductions
389 in SWA. Instead, they are often followed by high-frequency power increases that look like
390 'micro-arousals' (Fig. 9) according to sleep scoring criteria (Iber et al., 2007).
391
392 We then asked whether the high-frequency increases following type I slow waves differed
393 between DE, DEWR and NE. We found that type I slow waves induced significantly stronger
394 increases in high-frequency activity (18-30 Hz) in central regions (with a right-sided

JNeurosci Accepted Manuscript

lateralization) when subjects could recall the content of the dream (DE) as opposed to when they could not (DEWR, Fig. 10).

Spindles and dreaming

Finally, we examined how sleep spindles relate to dreaming. Similarly to the slow wave analysis, we applied a spindle detection algorithm (Ferrarelli et al., 2007) to the EEG signal, extracted spindle density, amplitude (maximum negative peak) and frequency, and averaged these parameters across all the spindles preceding each NREM awakening (stages N2 and N3). Based on previous studies supporting the existence of fast centro-parietal and slower frontal spindles (Anderer et al., 2001; De Gennaro and Ferrara, 2003; Andrillon et al., 2011), we separated spindles into slow and fast spindles using an individualized threshold (Siclari et al., 2014) (the intermediate value between the average spindle frequency in one centro-parietal (Pz) and one frontal (Fz) channel in each subject). We found that spindles preceding DE, compared to NE, were more numerous and had a higher frequency (Fig. 11). There were significantly more fast spindles preceding reports of DE, and these differences were relatively diffuse. However, a contrast between DEWR with NE showed that dreaming per se, (irrespective of the ability to the recall the content of the dream), was associated with significantly more fast spindles and fewer slow spindles in a central posterior region of the brain. The DE vs DEWR contrast did not show any significant differences (not shown).

Discussion

Slow wave characteristics and dreaming

JNeurosci Accepted Manuscript

The EEG slow wave of sleep occurs when thalamocortical neurons become bistable and start to oscillate between two states, each lasting a few hundred milliseconds: a hyperpolarized 'down-state', during which neurons are silent (off-period), and a depolarized 'up-state' ('on-period') characterized by neuronal firing (Steriade et al., 2001; Nir et al., 2011). In the present study we were able to link specific slow wave characteristics to dream experiences. We found that dreaming, as opposed to unconsciousness, was associated with fewer slow waves, which were smaller and shallower, and had a tendency to display a larger number of negative peaks. Large-scale computer simulations (Esser et al., 2007), local field potential studies in rodents (Vyazovskiy et al., 2007) and EEG studies in humans (Riedner et al., 2007) have revealed that the amplitude of slow waves reflects the number of neuronal populations that simultaneously enter a down-state and are thus in phase with each other, while the first and second slope of the slow waves are a measure of the speed with which neuronal populations transition into the down- and up-state, respectively. Finally, the number of negative peaks of a slow wave is related to the spatial synchrony of slow wave generation, with multipeak slow waves resulting from an asynchronous generation of slow waves in distant cortical regions. Our findings thus indicate that reports of no experience (unconsciousness) are more likely when large neuronal populations simultaneously and rapidly enter a down-state that is synchronized across central posterior cortical regions. Several studies have suggested that the off-period associated with slow waves represents the fundamental mechanism by which consciousness is lost during sleep. It has been shown that the slow-wave-like response induced by TMS during sleep leads to a break-down of cortical effective connectivity among specialized thalamocortical regions (Massimini et al., 2005; Massimini et al., 2010), thereby impairing information integration, which has been proposed as a prerequisite for consciousness (Tononi, 2008). The neuronal off-period associated with the slow-wave-like response to cortical stimulation leads to an interruption of deterministic interactions,

JNeurosci Accepted Manuscript

443 indicated by the loss of causal effects between the stimulation and brain activity resuming after
444 the off-period (measured by a phase locking index) (Pigorini et al., 2015). Our results are also
445 consistent with a previous study showing that within NREM sleep, TMS applied to posterior
446 cortical regions evokes a larger negative deflection and a shorter phase-locked response when
447 subjects reported unconsciousness compared to when they reported dreaming (Nieminen et al.,
448 2016).
449
450 *Topographical distribution of slow waves and dreaming*
451 Differences in slow wave characteristics between dreaming and unconsciousness, especially
452 amplitude and slope, were not uniformly distributed across the cortical surface, but were most
453 consistent in central and posterior regions. This is in line with our recent study, in which we
454 showed that dream reports were preceded by lower SWA in a posterior 'hot zone' of the brain,
455 comprising the medial and lateral occipital lobe and extending superiorly to the precuneus and
456 posterior cingulate gyrus (Siclari et al., 2017). Several imaging modalities converge to indicate
457 that the posterior cingulate gyrus is one of the most consistent cerebral 'hubs', connecting many
458 different brain areas (de Pasquale et al., 2017). The occurrence of off-states in this region may
459 thus lead to a breakdown of consciousness because it may disrupt connectivity with many
460 relatively distant areas of the brain. These results are also in line with reports of cessation of
461 dreaming after lesions of the inferior parietal and occipital cortex (Wilbrand; Murri et al., 1985;
462 Solms, 1997; Bischof and Bassetti, 2004), and with the observation that in the course of
463 development, dreaming appears to be closely related with the maturation of visuo-spatial skills,
464 which depend on posterior (parietal) cortical areas (Foulkes, 1999). In the frontal cortex on the
465 other hand, slow waves were less consistently associated with unconsciousness than in central
466 and posterior brain regions. When considering high-amplitude slow waves, we even found that

JNeurosci Accepted Manuscript

467 the opposite was true: these high-amplitude slow waves were larger and steeper in frontal regions
468 when they preceded reports of dream experiences.
469
470 *Type I and type II slow waves*
471 We recently obtained evidence for two types of synchronization processes underlying slow waves
472 in the transition to sleep: a presumably subcortico-cortical synchronization process giving rise to
473 isolated, very large and steep slow waves with a fronto-central involvement (type I slow waves),
474 and a presumably cortico-cortical synchronization process underlying smaller slow waves, with
475 more variable cortical origins (type II slow waves) (Siclari et al., 2014). These two processes are
476 temporally dissociated in the falling asleep period in adults, but are also present during stable
477 sleep (Bernardi et al.). The fact that reports of dreaming are particularly likely when large, steep
478 and frontal type I slow waves occur could be explained by several findings. First, type I slow
479 waves are more likely to be large and steep when they occur on an EEG background of low SWA
480 (Fig. 8C). Therefore, the presence of frontal type I slow waves may indicate that most cortical
481 regions, and in particular posterior areas, are in a state of relatively low bistability and are more
482 likely to contribute to conscious experiences. Second, several lines of evidence suggest that type I
483 slow waves may be related to arousal systems. Source modeling analyses have revealed that they
484 originate preferentially in sensorimotor regions and in the posterior-medial parietal cortex, and
485 that they involve primarily fronto-medial regions (Siclari et al., 2014). The regions of origin are
486 the brain areas with the highest noradrenergic innervation in the human and monkey cortex
487 (Gaspar et al., 1989; Javoy-Agid et al., 1989; Lewis and Morrison, 1989). Cortical projections
488 targeting preferentially the frontal medial area, consistent with the medial frontal involvement,
489 have been described for the pontine and mesencephalic reticular formation (Jones and Yang,
490 1985), another arousal-promoting structure, and the ventromedial thalamic nucleus (Desbois and

JNeurosci Accepted Manuscript

Villanueva, 2001; Kuramoto et al., 2015). Very large amplitude slow waves are specifically associated with fMRI brain stem activations including the locus coeruleus (Dang-Vu et al., 2008), and it is well known that K-complexes, which share many properties with type I slow waves (Siclari et al., 2014), can be induced by peripheral sensory stimulations. Finally, type I slow waves tend to be followed by increases in high-frequency spectral power that peak in fronto-medial regions (Fig. 8E), often fulfill the criteria for "micro-arousals" (Iber et al., 2007)(Fig. 9), and herald successful recall of dream content (Fig. 10). The topographic distribution of these high-frequency increases (Fig 8D) closely matches the distribution of high-frequency activity that has previously been shown to distinguish dreams with and without recalled dream content (Siclari et al., 2017). Interestingly and in line with these findings, intrasleep awakenings are higher in frequent dream recallers compared to infrequent dream recallers (Ruby et al., 2013; Eichenlaub et al., 2014). Increases in high-frequency power may thus reflect the intermittent activation of arousal systems and in particular surges in noradrenergic activity occurring in NREM sleep (Aston-Jones and Bloom, 1981). Notably, noradrenaline favors memory encoding and consolidation in both wakefulness (Roozendaal and McGaugh, 2011) and sleep (Gais et al., 2011).

Spindles and dreaming

Our findings suggest that dreaming is more likely to occur in the presence of fast spindles in a central and posterior cortical region, while reports of no experience preferentially occur in the presence of slow spindles in the same areas. These findings are consistent with the recent observation that subjects who reported a high number of dreams had faster spindles (Nielsen, 2016). Spindle frequency has been related to the level of thalamic hyperpolarization and typically decreases in the course of the falling asleep period (Himanen et al., 2002; Andrillon et al., 2011;

JNeurosci Accepted Manuscript

515 Siclari et al., 2014), along with increasing levels of thalamic hyperpolarization (Andrillon et al.,
516 2011) and SWA. One possibility is that these findings indirectly reflect differences in slow wave
517 characteristics. Spindles occurring during the positive to negative deflection of the slow wave
518 (progressive cortical hyperpolarization) tend to be slower than spindles occurring during the
519 negative-to-positive phase of the EEG slow wave (transition to depolarized cortical up-state)
520 (Molle et al., 2011; Siclari et al., 2014). It is thus conceivable that when slow waves are sparse
521 and shallow and are associated with longer up-states, fast spindles are more likely to occur. The
522 fact that both slow wave and spindle differences were most consistent over the same posterior
523 brain areas would support such an interpretation.
524
525 *Limitations*
526 It should be noted that our distinction between type I and type II slow waves, although supported
527 by different observations, is based on an arbitrary cutoff, as there is currently no better way to
528 separate the two types of slow waves in stable sleep. Therefore, future studies using techniques
529 allowing to directly image arousal-related subcortical structures will be necessary to validate this
530 separation and the results.
531
532 *Summary and conclusions*
533 Here we show that dreaming in NREM sleep is determined by the proportion and distribution of
534 two distinct types of slow waves. Dream experiences are more likely to occur when the majority
535 of slow waves (type II slow waves) are small, sparse and shallow, especially in posterior brain
536 regions. The content of dream experiences is more likely to be reported if, in addition, high-
537 amplitude slow waves (type I slow waves) occur in fronto-central brain regions and are followed
538 by high-frequency increases (local 'micro-arousals'). These results suggest that the capacity of

JNeurosci Accepted Manuscript

539 the brain to generate experiences during sleep is reduced in the presence of large type II slow
540 waves in posterior and central brain regions, and that dream recall may be facilitated by the
541 intermittent activation of arousal systems during NREM sleep (associated with type I slow
542 waves).

543
544
545
546
547 **References**

548

549 Anderer P, Klosch G, Gruber G, Trenker E, Pascual-Marqui RD, Zeitlhofer J, Barbanoj MJ,
550 Rappelsberger P, Saletu B (2001) Low-resolution brain electromagnetic tomography
551 revealed simultaneously active frontal and parietal sleep spindle sources in the human
552 cortex. Neuroscience 103:581-592.
553 Andrillon T, Nir Y, Staba RJ, Ferrarelli F, Cirelli C, Tononi G, Fried I (2011) Sleep spindles in
554 humans: insights from intracranial EEG and unit recordings. J Neurosci 31:17821-17834.
555 Antrobus J, Kondo T, Reinsel R, Fein G (1995) Dreaming in the late morning: summation of
556 REM and diurnal cortical activation. Conscious Cogn 4:275-299.
557 Aserinsky E, Kleitman N (1955) Two types of ocular motility occuring during sleep. J Appl
558 Physiol 8:11-18.
559 Aston-Jones G, Bloom FE (1981) Activity of norepinephrine-containing locus coeruleus neurons
560 in behaving rats anticipates fluctuations in the sleep-waking cycle. J Neurosci 1:876-886.
561 Bernardi G, Siclari F, Handjaras G, Riedner BA, Tononi G (2018) Local and widespread slow
562 waves in stable NREM sleep: evidence for distinct regulation mechanisms. Front Human
563 Neurosci, *in press*.

JNeurosci Accepted Manuscript

564 Bernardi G, Cecchetti L, Siclari F, Buchmann A, Yu X, Handjaras G, Bellesi M, Ricciardi E,
565 Kecskemeti SR, Riedner BA, Alexander AL, Benca RM, Ghilardi MF, Pietrini P, Cirelli
566 C, Tononi G (2016) Sleep reverts changes in human gray and white matter caused by
567 wake-dependent training. Neuroimage 129:367-377.
568 Bischof M, Bassetti CL (2004) Total dream loss: a distinct neuropsychological dysfunction after
569 bilateral PCA stroke. Ann Neurol 56:583-586.
570 Chellappa SL, Frey S, Knoblauch V, Cajochen C (2011) Cortical activation patterns herald
571 successful dream recall after NREM and REM sleep. Biol Psychol 87:251-256.
572 Dang-Vu TT, Schabus M, Desseilles M, Albouy G, Boly M, Darsaud A, Gais S, Rauchs G,
573 Sterpenich V, Vandewalle G, Carrier J, Moonen G, Balteau E, Degueldre C, Luxen A,
574 Phillips C, Maquet P (2008) Spontaneous neural activity during human slow wave sleep.
575 Proc Natl Acad Sci U S A 105:15160-15165.
576 De Gennaro L, Ferrara M (2003) Sleep spindles: an overview. Sleep Med Rev 7:423-440.
577 de Pasquale F, Corbetta M, Betti V, Della Penna S (2017) Cortical cores in network dynamics.
578 Neuroimage.
579 Delorme A, Makeig S (2004) EEGLAB: an open source toolbox for analysis of single-trial EEG
580 dynamics including independent component analysis. J Neurosci Methods 134:9-21.
581 Desbois C, Villanueva L (2001) The organization of lateral ventromedial thalamic connections in
582 the rat: a link for the distribution of nociceptive signals to widespread cortical regions.
583 Neuroscience 102:885-898.
584 Eichenlaub JB, Bertrand O, Morlet D, Ruby P (2014) Brain reactivity differentiates subjects with
585 high and low dream recall frequencies during both sleep and wakefulness. Cereb Cortex
586 24:1206-1215.

JNeurosci Accepted Manuscript

587 Esposito MJ, Nielsen TA, Paquette T (2004) Reduced Alpha power associated with the recall of
588 mentation from Stage 2 and Stage REM sleep. Psychophysiology 41:288-297.
589 Esser SK, Hill SL, Tononi G (2007) Sleep homeostasis and cortical synchronization: I. Modeling
590 the effects of synaptic strength on sleep slow waves. Sleep 30:1617-1630.
591 Ferrarelli F, Huber R, Peterson MJ, Massimini M, Murphy M, Riedner BA, Watson A, Bria P,
592 Tononi G (2007) Reduced sleep spindle activity in schizophrenia patients. Am J
593 Psychiatry 164:483-492.
594 Foulkes D (1999) Children's dreaming and the development of consciousness. Cambridge, MA:
595 Harvard University Press.
596 Funk CM, Honjoh S, Rodriguez AV, Cirelli C, Tononi G (2016) Local Slow Waves in
597 Superficial Layers of Primary Cortical Areas during REM Sleep. Curr Biol 26:396-403.
598 Gais S, Rasch B, Dahmen JC, Sara S, Born J (2011) The memory function of noradrenergic
599 activity in non-REM sleep. J Cogn Neurosci 23:2582-2592.
600 Gaspar P, Berger B, Febvret A, Vigny A, Henry JP (1989) Catecholamine innervation of the
601 human cerebral cortex as revealed by comparative immunohistochemistry of tyrosine
602 hydroxylase and dopamine-beta-hydroxylase. J Comp Neurol 279:249-271.
603 Himanen SL, Virkkala J, Huhtala H, Hasan J (2002) Spindle frequencies in sleep EEG show U-
604 shape within first four NREM sleep episodes. J Sleep Res 11:35-42.
605 Huber R, Ghilardi MF, Massimini M, Tononi G (2004) Local sleep and learning. Nature 430:78-
606 81.
607 Iber C, Ancoli-Israel S, Chesson A, Quan SF (2007) The AASM Manual for the Scoring of Sleep
608 and Associated Events: Rules, Terminology and Technical Specifications, 1st Edition.
609 Westchester, Illinois: American Academy of Sleep Medicine.

JNeurosci Accepted Manuscript

610 Javoy-Agid F, Scatton B, Ruberg M, L'Heureux R, Cervera P, Raisman R, Maloteaux JM, Beck
611 H, Agid Y (1989) Distribution of monoaminergic, cholinergic, and GABAergic markers
612 in the human cerebral cortex. Neuroscience 29:251-259.
613 Jones BE, Yang TZ (1985) The efferent projections from the reticular formation and the locus
614 coeruleus studied by anterograde and retrograde axonal transport in the rat. J Comp
615 Neurol 242:56-92.
616 Jung TP, Makeig S, Humphries C, Lee TW, McKeown MJ, Iragui V, Sejnowski TJ (2000)
617 Removing electroencephalographic artifacts by blind source separation.
618 Psychophysiology 37:163-178.
619 Kuramoto E, Ohno S, Furuta T, Unzai T, Tanaka YR, Hioki H, Kaneko T (2015) Ventral medial
620 nucleus neurons send thalamocortical afferents more widely and more preferentially to
621 layer 1 than neurons of the ventral anterior-ventral lateral nuclear complex in the rat.
622 Cereb Cortex 25:221-235.
623 Lewis DA, Morrison JH (1989) Noradrenergic innervation of monkey prefrontal cortex: a
624 dopamine-beta-hydroxylase immunohistochemical study. J Comp Neurol 282:317-330.
625 Marzano C, Ferrara M, Mauro F, Moroni F, Gorgoni M, Tempesta D, Cipolli C, De Gennaro L
626 (2011) Recalling and forgetting dreams: theta and alpha oscillations during sleep predict
627 subsequent dream recall. J Neurosci 31:6674-6683.
628 Massimini M, Ferrarelli F, Huber R, Esser SK, Singh H, Tononi G (2005) Breakdown of cortical
629 effective connectivity during sleep. Science 309:2228-2232.
630 Massimini M, Ferrarelli F, Murphy M, Huber R, Riedner B, Casarotto S, Tononi G (2010)
631 Cortical reactivity and effective connectivity during REM sleep in humans. Cogn
632 Neurosci 1:176-183.

JNeurosci Accepted Manuscript

633 Molle M, Bergmann TO, Marshall L, Born J (2011) Fast and slow spindles during the sleep slow
634 oscillation: disparate coalescence and engagement in memory processing. Sleep 34:1411-
635 1421.
636 Monroe LJ, Rechtschaffen A, Foulkes D, Jensen J (1965) Discriminability of Rem and Nrem
637 Reports. J Pers Soc Psychol 12:456-460.
638 Murri L, Massetani R, Siciliano G, Giovanditti L, Arena R (1985) Dream recall after sleep
639 interruption in brain-injured patients. Sleep 8:356-362.
640 Nichols TE, Holmes AP (2002) Nonparametric permutation tests for functional neuroimaging: a
641 primer with examples. Hum Brain Mapp 15:1-25.
642 Nielsen T, Carr, M., Blanchette-Carrière, C., Marquis, L., Dumel, G., Solomonova, E., Julien, S.,
643 Picard-Deland, C., Paquette, T. (2016) NREM sleep spindles are associated with dream
644 recall. Sleep Spindles & Cortical Up States 1:27-41.
645 Nieminen JO, Gosseries O, Massimini M, Saad E, Sheldon AD, Boly M, Siclari F, Postle BR,
646 Tononi G (2016) Consciousness and cortical responsiveness: a within-state study during
647 non-rapid eye movement sleep. Sci Rep 6:30932.
648 Nir Y, Staba RJ, Andrillon T, Vyazovskiy VV, Cirelli C, Fried I, Tononi G (2011) Regional slow
649 waves and spindles in human sleep. Neuron 70:153-169.
650 Oudiette D, Dealberto MJ, Uguccioni G, Golmard JL, Merino-Andreu M, Tafti M, Garma L,
651 Schwartz S, Arnulf I (2012) Dreaming without REM sleep. Conscious Cogn 21:1129-
652 1140.
653 Pigorini A, Sarasso S, Proserpio P, Szymanski C, Arnulfo G, Casarotto S, Fecchio M, Rosanova
654 M, Mariotti M, Lo Russo G, Palva JM, Nobili L, Massimini M (2015) Bistability breaks-
655 off deterministic responses to intracortical stimulation during non-REM sleep.
656 Neuroimage 112:105-113.

JNeurosci Accepted Manuscript

657 Riedner BA, Vyazovskiy VV, Huber R, Massimini M, Esser S, Murphy M, Tononi G (2007)
658 Sleep homeostasis and cortical synchronization: III. A high-density EEG study of sleep
659 slow waves in humans. Sleep 30:1643-1657.
660 Roozendaal B, McGaugh JL (2011) Memory modulation. Behav Neurosci 125:797-824.
661 Ruby P, Blochet C, Eichenlaub JB, Bertrand O, Morlet D, Bidet-Caulet A (2013) Alpha
662 reactivity to first names differs in subjects with high and low dream recall frequency.
663 Front Psychol 4:419.
664 Siclari F, Larocque JJ, Postle BR, Tononi G (2013) Assessing sleep consciousness within
665 subjects using a serial awakening paradigm. Front Psychol 4:542.
666 Siclari F, Bernardi G, Riedner B, LaRocque J, Benca MR, Tononi G (2014) Two distinct
667 synchronization processes in the transition to sleep: a high-density
668 electroencephalographic study. Sleep 37:1621-1637.
669 Siclari F, Baird B, Perogamvros L, Bernardi G, LaRocque JJ, Riedner B, Boly M, Postle BR,
670 Tononi G (2017) The neural correlates of dreaming. Nat Neurosci 20:872-878.
671 Solms M (1997) The neuropsychology of dreams: a clinico-anatomical study. Mahwah, NJ:
672 Erlbaum.
673 Solms M (2000) Dreaming and REM sleep are controlled by different brain mechanisms. Behav
674 Brain Sci 23:843-850; discussion 904-1121.
675 Steriade M, Timofeev I, Grenier F (2001) Natural waking and sleep states: a view from inside
676 neocortical neurons. J Neurophysiol 85:1969-1985.
677 Stickgold R, Malia A, Fosse R, Propper R, Hobson JA (2001) Brain-mind states: I. Longitudinal
678 field study of sleep/wake factors influencing mentation report length. Sleep 24:171-179.
679 Tononi G (2008) Consciousness as integrated information: a provisional manifesto. Biol Bull
680 215:216-242.

JNeurosci Accepted Manuscript

681 Vyazovskiy VV, Riedner BA, Cirelli C, Tononi G (2007) Sleep homeostasis and cortical
682 synchronization: II. A local field potential study of sleep slow waves in the rat. Sleep
683 30:1631-1642.
684 Wilbrand H Ein Fall von Seelenblindheit und Hemianopsie mit Sektionsbefund. Deutsche
685 Zeitschrift für Nervenheilkunde 2:361-387.
686 Williamson PC, Csima A, Galin H, Mamelak M (1986) Spectral EEG correlates of dream recall.
687 Biol Psychiatry 21:717-723.

688
689
690
691
692
693
694
695
696
697
698
699

700 **Figure legends**

701

702 **Figure 1**. Top row: Topographical distribution of t values for the contrast between dream
703 experiences and no experiences for different slow wave parameters averaged over the last 60s

JNeurosci Accepted Manuscript

before the awakening. Bottom row: same as top row but electrodes within a cluster showing a statistically significant effect are marked in white ($p < 0.05$, cluster-based correction for multiple comparisons, two-tailed paired *t*-tests, $n = 12$ subjects).

Figure 2. Top row: Topographical distribution of slow wave parameters for dream experiences (DE, first row) and no experience (NE, second row). Slow wave parameters were averaged over the 60 last seconds before the awakening and across 12 subjects. In the third row, mean differences between DE and NE (DE minus NE) are shown for each parameter, so that red colors indicate higher values in DE, and blue colors higher values in NE. In the fourth row, p-values for paired electrode-by-electrode t-tests are shown ($p<0.05$, uncorrected).

Figure 3. Top row: Topographical distribution of t values for the contrast between dream experiences without recall of content and no experiences for different slow wave parameters averaged over the last 60s before the awakening. Bottom row: same as Top row but electrodes within a cluster showing a statistically significant effect are marked in white ($p < 0.05$, cluster-based correction for multiple comparisons, two-tailed paired *t*-tests, $n = 12$ subjects).

Figure 4. Top row: Topographical distribution of t values for the contrast between dream experiences and no experiences for different slow wave parameters averaged over the last 60s before the awakening. For each subject, only slow waves larger than the 75^{th} amplitude percentile (across all slow waves detected in NREM sleep) were included. Bottom row: same as top row but electrodes within a cluster showing a statistically significant effect are now marked in white ($p < 0.05$, cluster-based correction for multiple comparisons, two-tailed paired *t*-tests, $n = 12$ subjects).

JNeurosci Accepted Manuscript

728

729 **Figure 5**. Top row: Topographical distribution of slow wave parameters for dream experiences
730 (DE, first row) and no experience (NE, second row). Slow wave parameters were averaged over
731 the 60 last seconds before the awakening and across 12 subjects. In the third row, mean
732 differences between DE and NE (DE minus NE) are shown for each parameter, so that red colors
733 indicate higher values in DE, and blue colors higher values in NE. In the fourth row, p-values for
734 paired electrode-by-electrode t-tests are shown ($p<0.05$, uncorrected). Here only slow waves
735 larger than the 75th amplitude percentile were included for each subject.

736

737 **Figure 6**. Top row: Topographical distribution of t values for the contrast between dream
738 experiences and dream experiences without recall of content for different slow wave parameters
739 averaged over the last 60s before the awakening. For each subject, only slow waves larger than
740 the 75th amplitude percentile were included. Bottom row: same as top row but electrodes within a
741 cluster showing a statistically significant effect are marked in white ($p < 0.05$, cluster-based
742 correction for multiple comparisons, $n = 14$ subjects).

743

744 **Figure 7.** Correlation between slow wave amplitude in a frontal and occipital region of interest
745 for two representative subjects. Top row. All slow waves (no amplitude threshold). Bottom row.
746 An amplitude threshold (above the 75th percentile of all waves for each subject) was applied to
747 frontal slow waves.

748

749 **Figure 8.** Type I and type II slow wave characteristics. **A**. Proportion of slow waves classified as
750 type I (left) or type II (right) based on synchronization efficiency that were also defined as large
751 based on the channel-by-channel amplitude criterion (>75th percentile; for comparison, slow

JNeurosci Accepted Manuscript

752 waves were identified in a 250 ms time-window centered on the peak of the type I/II slow wave).
753 Each bar in the graph represents the average (%) across subjects ± SD. **B.** Type I/type II ratio for
754 the 60s preceding DE, DEWR and NE (mean and standard error of the mean). Asterisks indicate
755 statistically significant differences at $p<0.05$ (paired two-tailed t-tests). **C**. Correlation between
756 low-frequency spectral power in the 1-4 Hz range (in the 6s preceding the slow wave) and the
757 synchronization index (reflecting slow wave amplitude and slope) for type I and type II slow
758 waves (Spearman rank correlation coefficient). Type I and type II slow waves were separated
759 according to their synchronization index (see method section for details). Electrodes within a
760 cluster showing a statistically significant effect are marked in white ($p < 0.05$, cluster-based
761 correction for multiple comparisons). **D**. Spectral power changes (%) induced by type I and type
762 II slow waves in a frontal electrode cluster (Fz and immediately neighboring electrodes). Spectral
763 power in the 6s following the slow wave was compared with spectral power in the 6s preceding
764 each slow wave for different frequency bands (1-40 Hz, resolution of 2 Hz bins). Bottom row: p-
765 values for the comparison between PSD changes induced by type I and type II slow waves
766 (paired two-tailed t-tests). **E**. Cortical distribution of spectral power changes in the 18-30 Hz for
767 type I slow waves at the source level.
768
769 **Figure 9**. Representative examples of high-frequency increases following type I slow waves.
770 Time 0 corresponds to the maximum negative peak of the type I slow wave. Four representative
771 midline channels are displayed (Fz, Cz, Pz and Oz), referenced to the average of two mastoid
772 channels.
773
774 **Figure 10**. Topographical distribution of t values for the contrast in 18-30 Hz changes induced by
775 type I slow waves between DE and NE (left), DE and DEWR (middle) and DEWR and NE

JNeurosci Accepted Manuscript

776 (right), averaged over the last 60s before the awakening. Electrodes within a cluster showing a
777 statistically significant effect are marked in white ($p < 0.05$, cluster-based correction for multiple
778 comparisons, two-tailed paired *t*-tests, n=12 subjects for DE, $n = 11$ subjects for NE, n=13
779 subjects for DEWR).
780
781 **Figure 11**: Top row: Topographical distribution of t values for the contrast between dream
782 experiences and no experiences for different spindle parameters (60s before awakening).
783 Electrodes within a cluster showing a statistically significant effect are marked in white ($p < 0.05$,
784 cluster-based correction for multiple comparisons, two-tailed paired *t*-tests, n =12 subjects) are
785 marked in white. Bottom row: same as top row for dream experiences without recall of content vs
786 no experience.
787
788
789

JNeurosci Accepted Manuscript

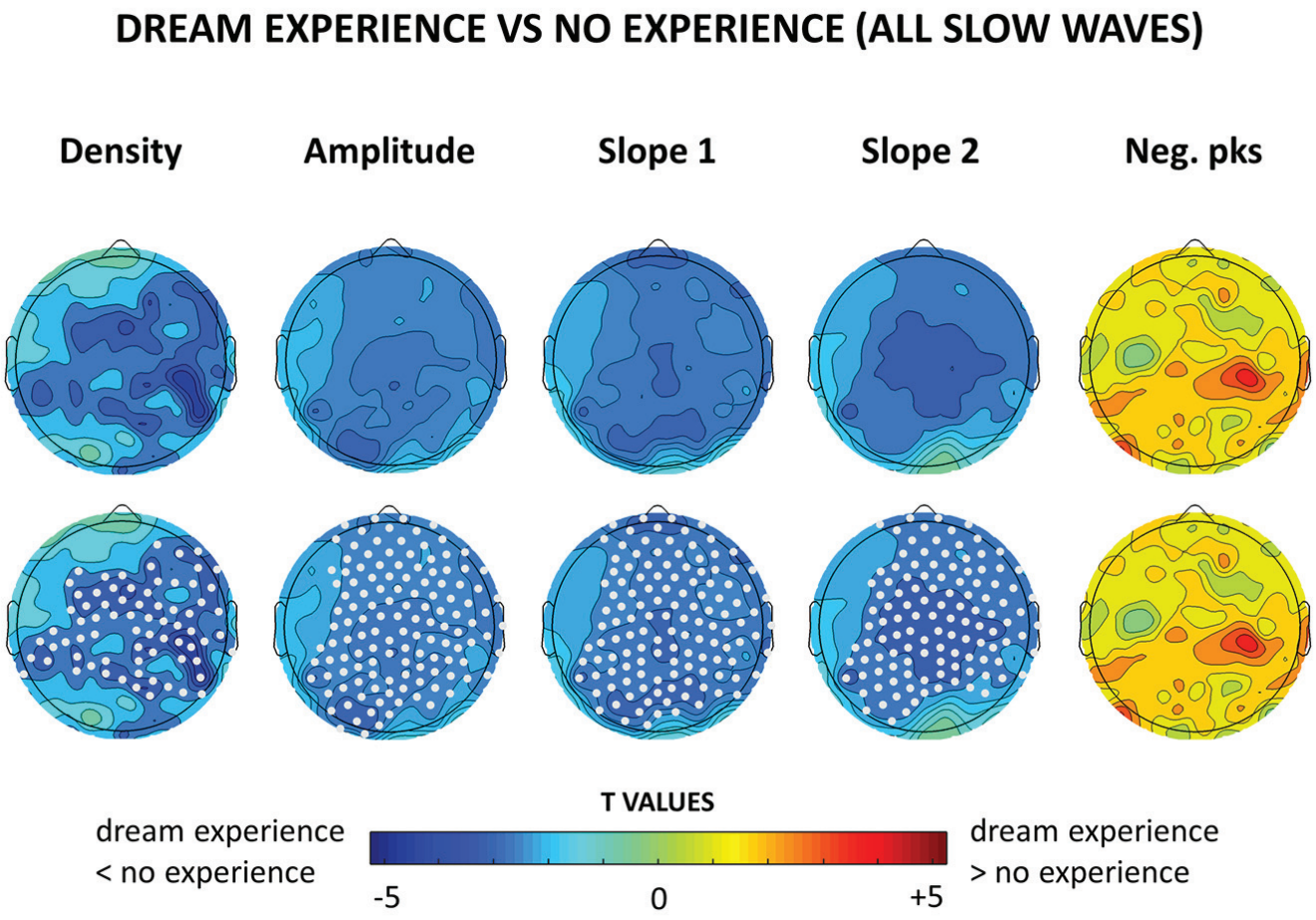

JNeurosci Accepted Manuscript

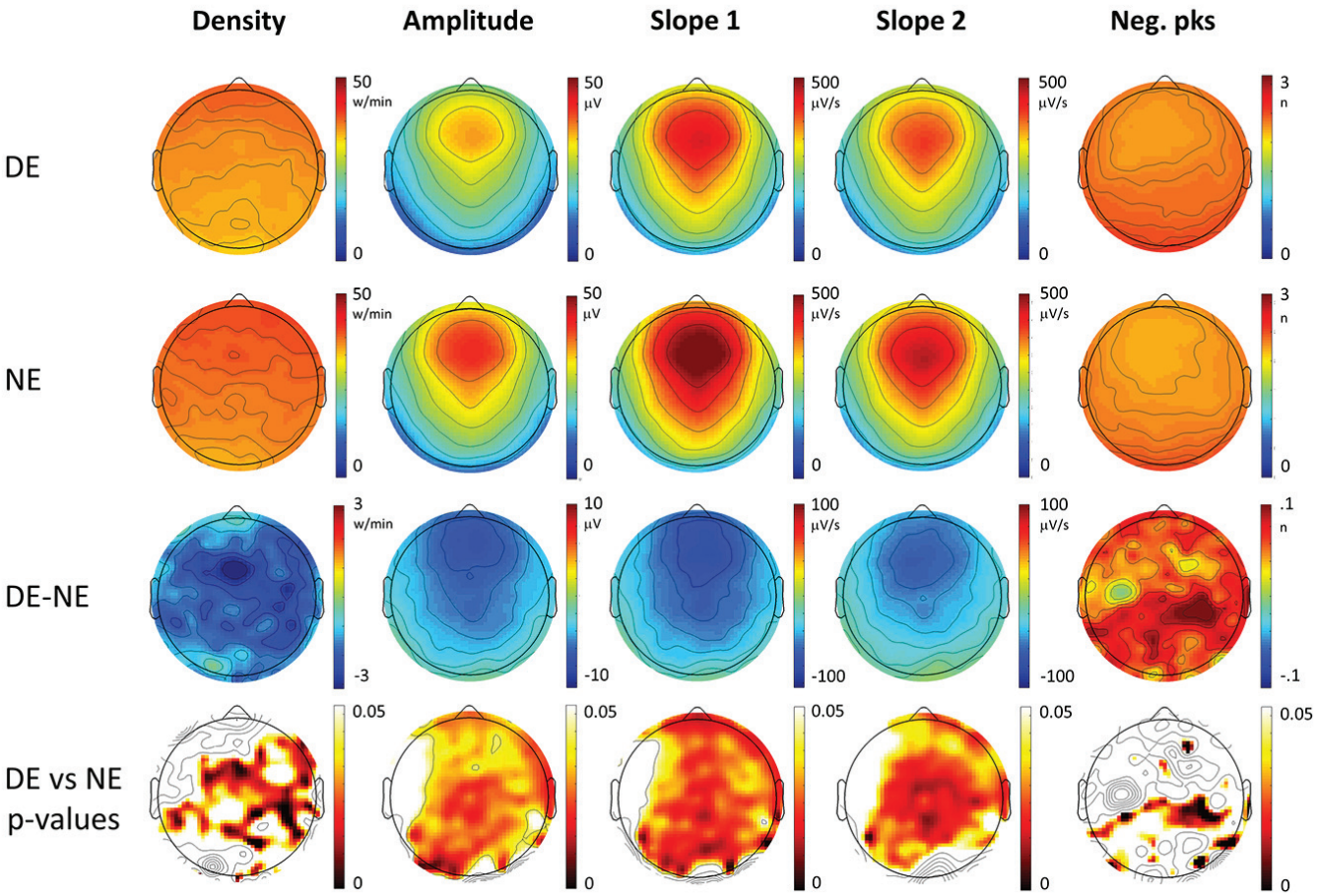

JNeurosci Accepted Manuscript

DREAM EXPERIENCE w/o RECALL of CONTENT VS NO EXPERIENCE (ALL SLOW WAVES)

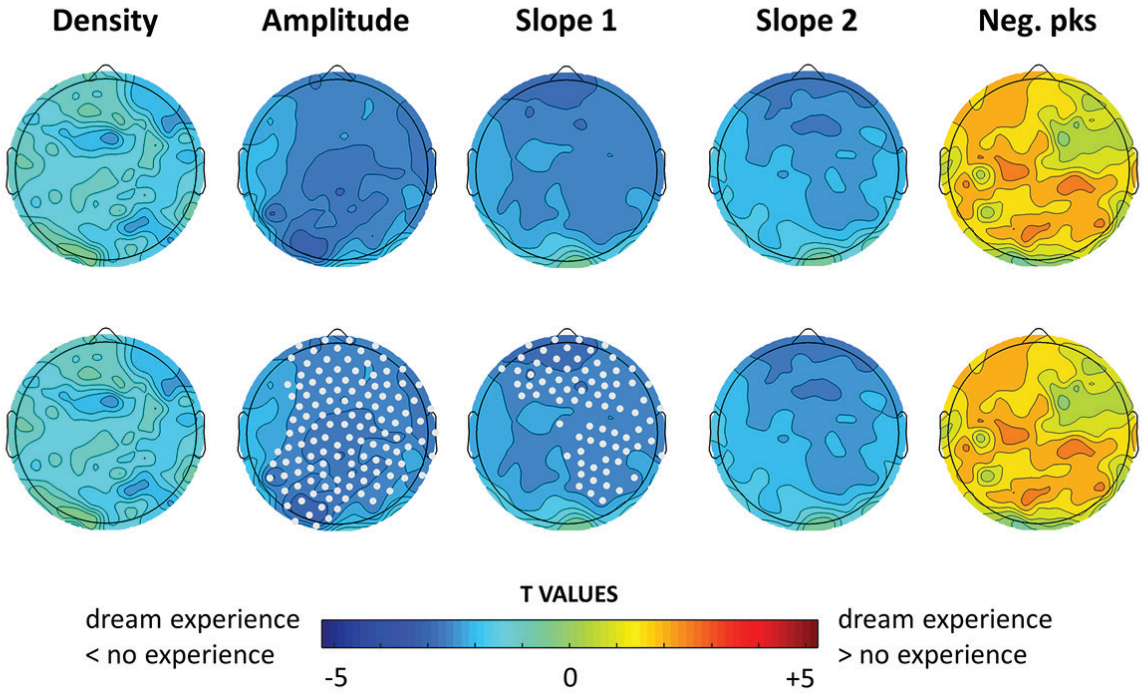

JNeurosci Accepted Manuscript

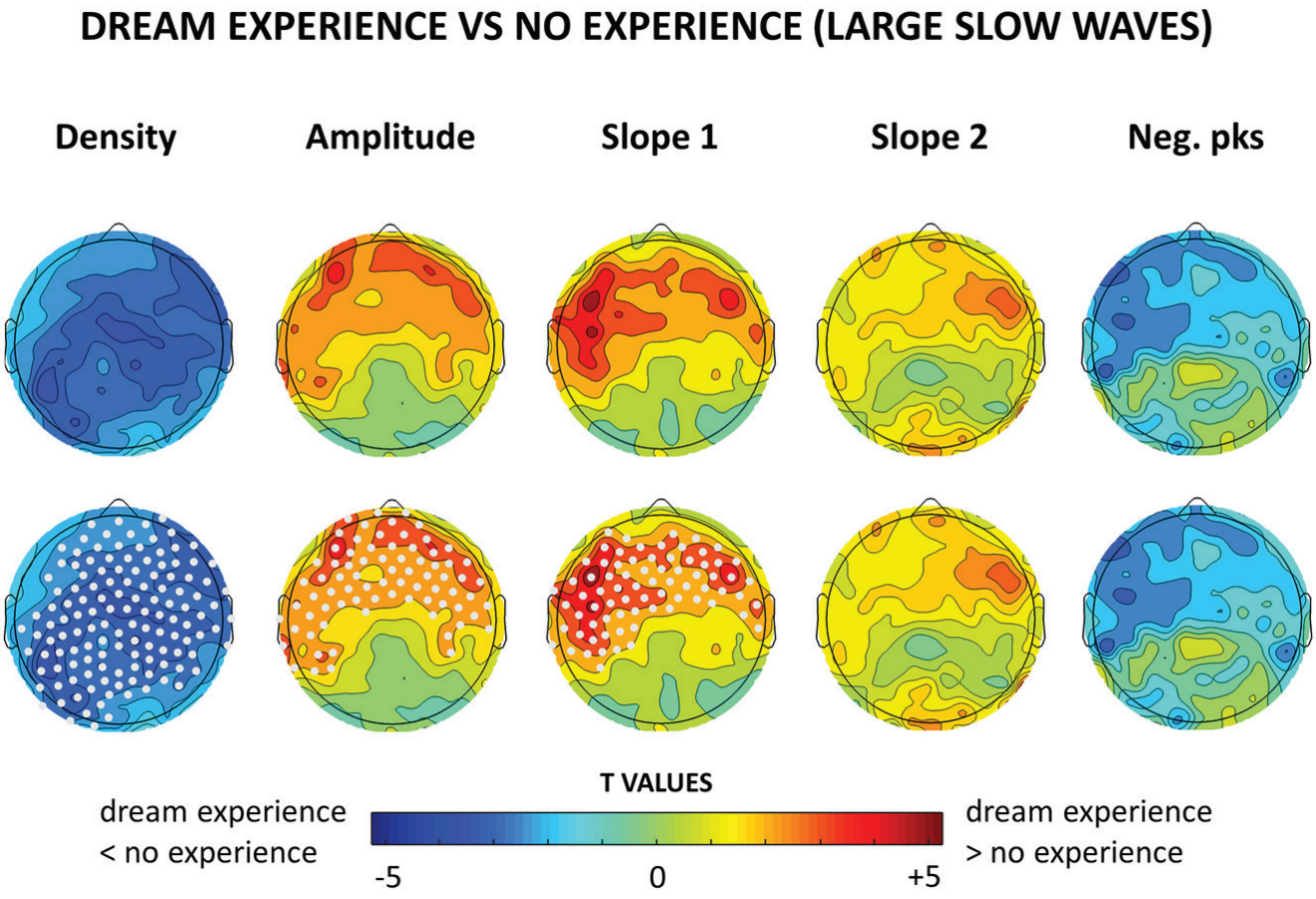

JNeurosci Accepted Manuscript

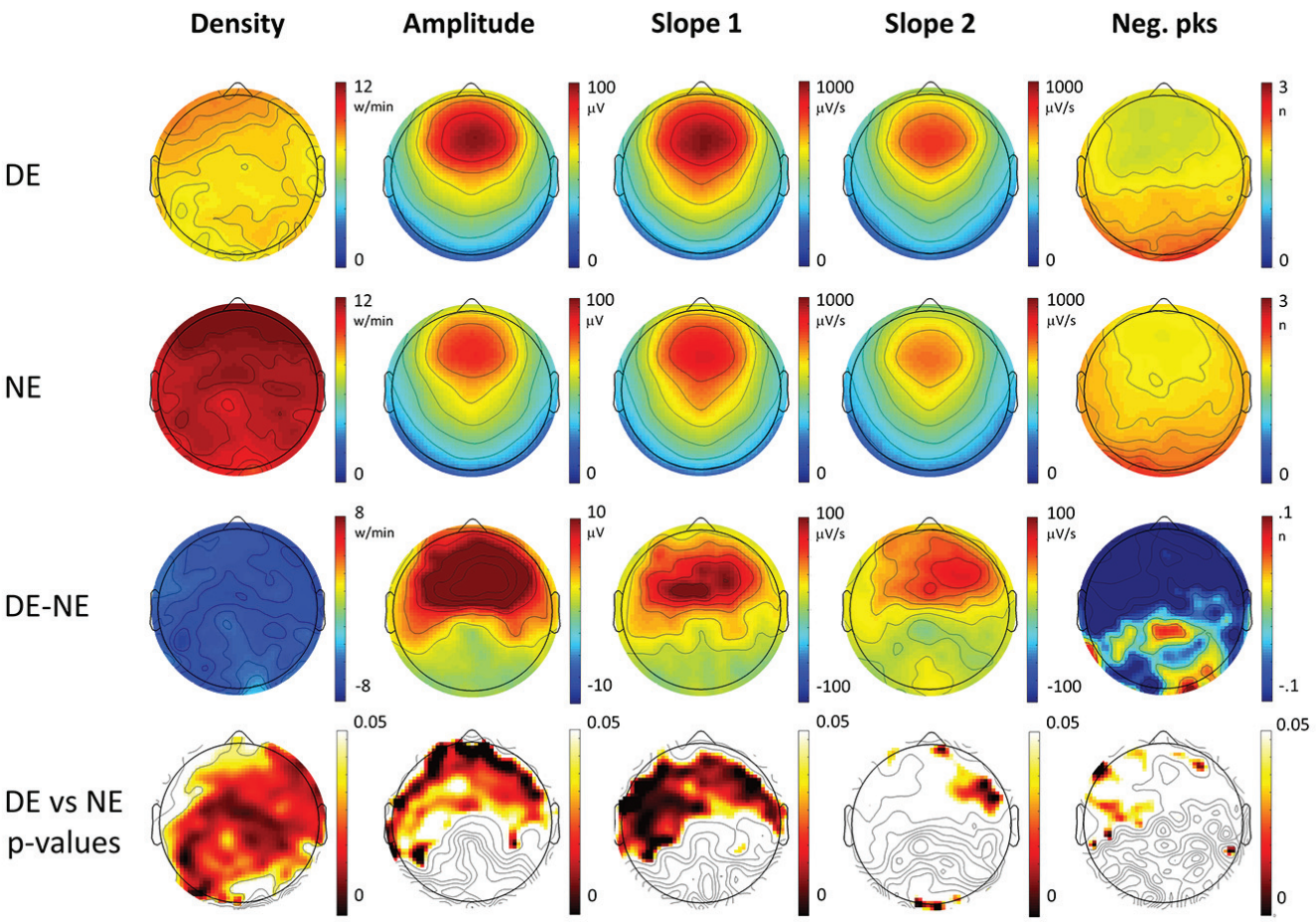

JNeurosci Accepted Manuscript

DREAM EXPERIENCE WITH VS. WITHOUT RECALL of CONTENT (LARGE SLOW WAVES)

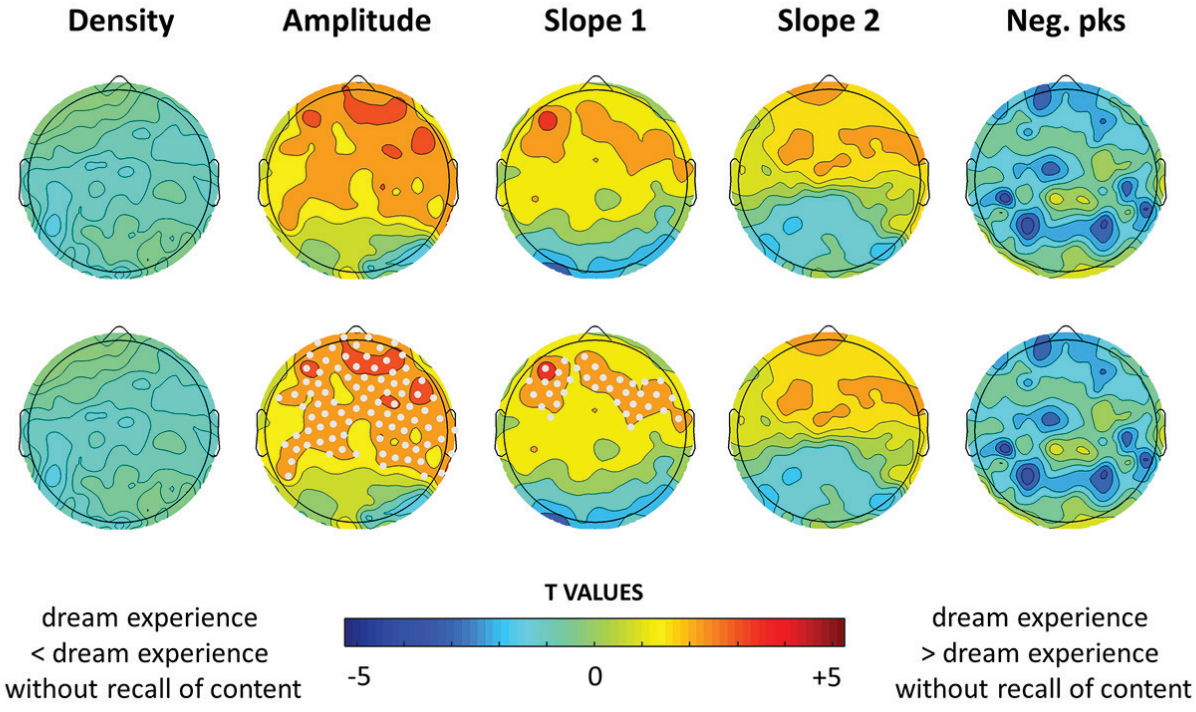

JNeurosci Accepted Manuscript

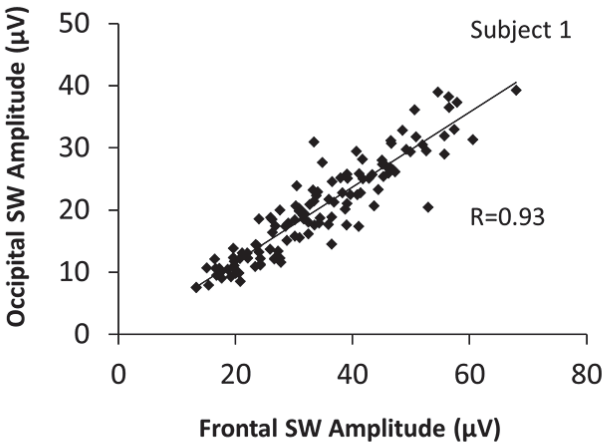

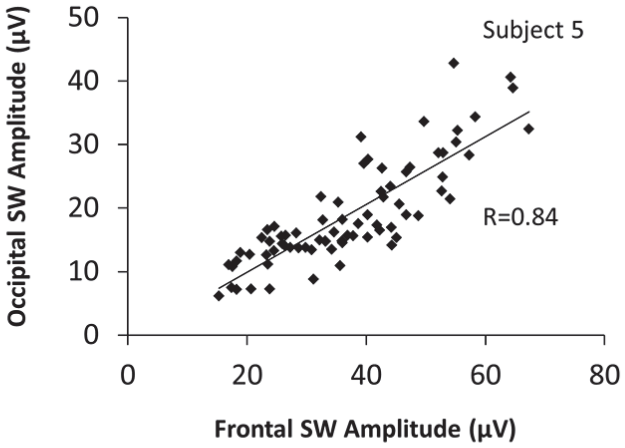

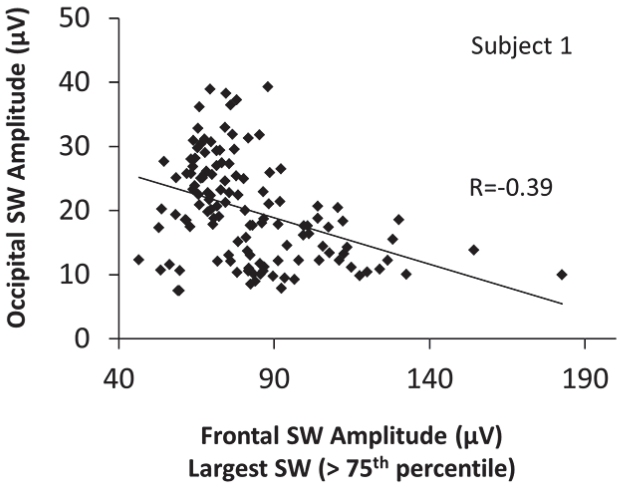

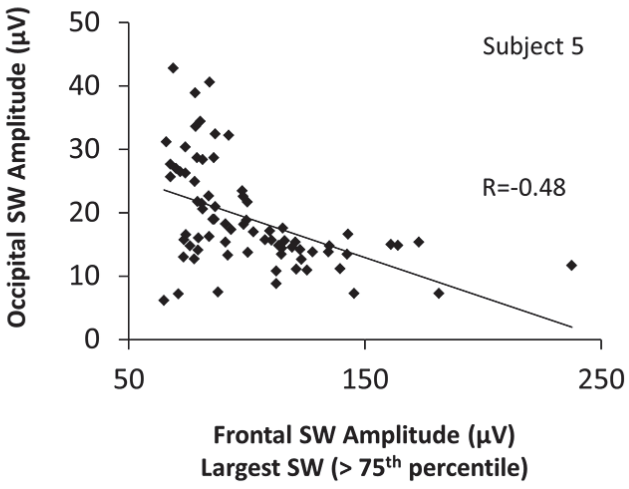

JNeurosci Accepted Manuscript

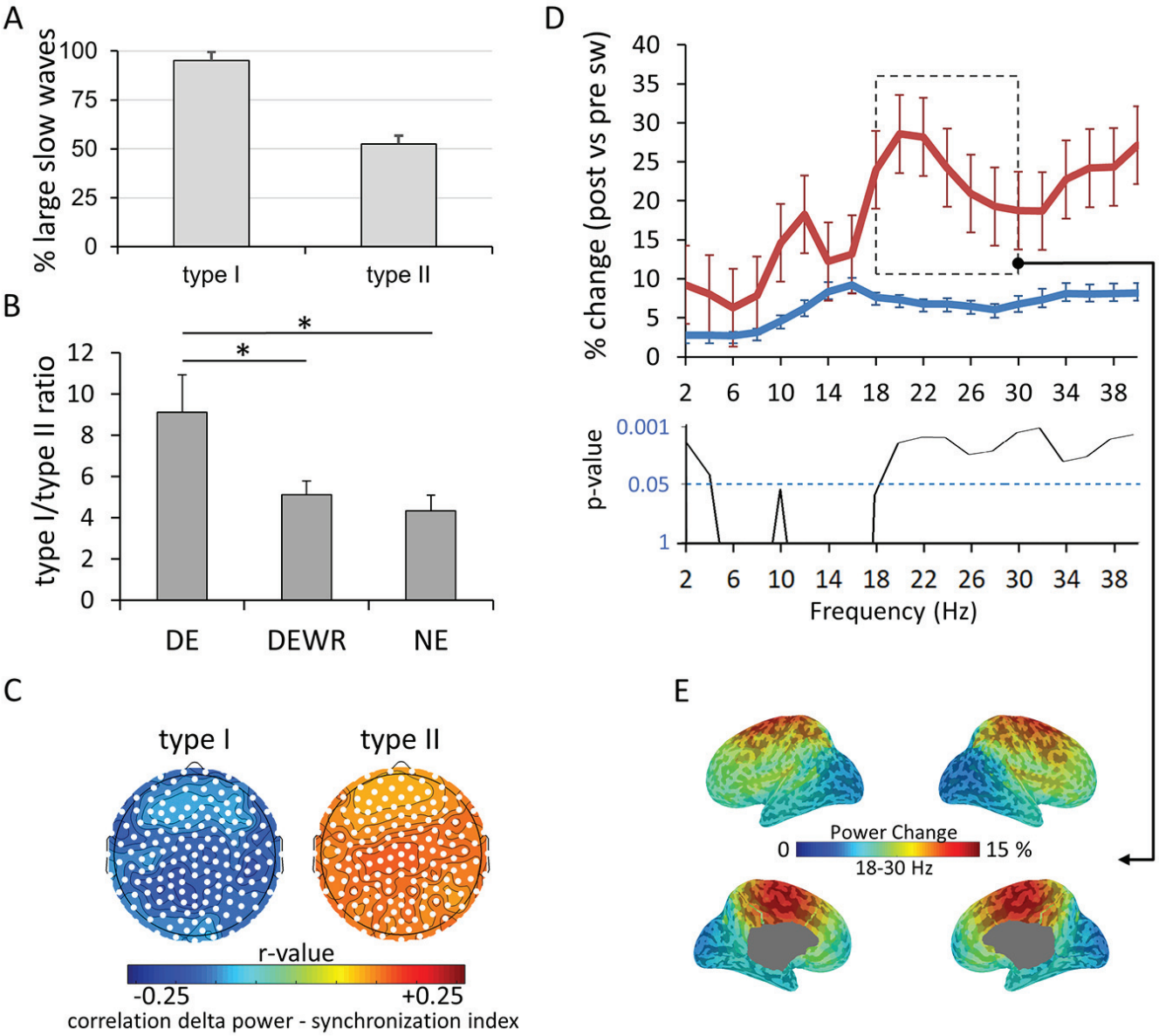

JNeurosci Accepted Manuscript

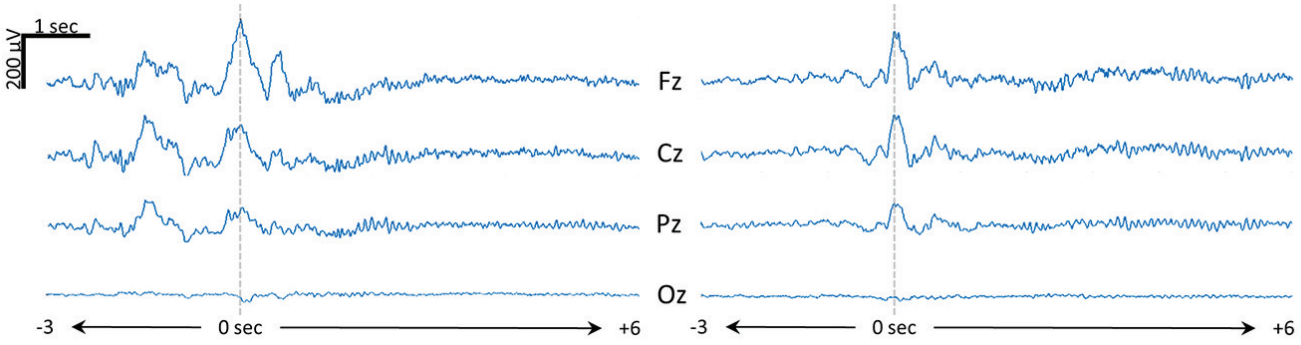

JNeurosci Accepted Manuscript

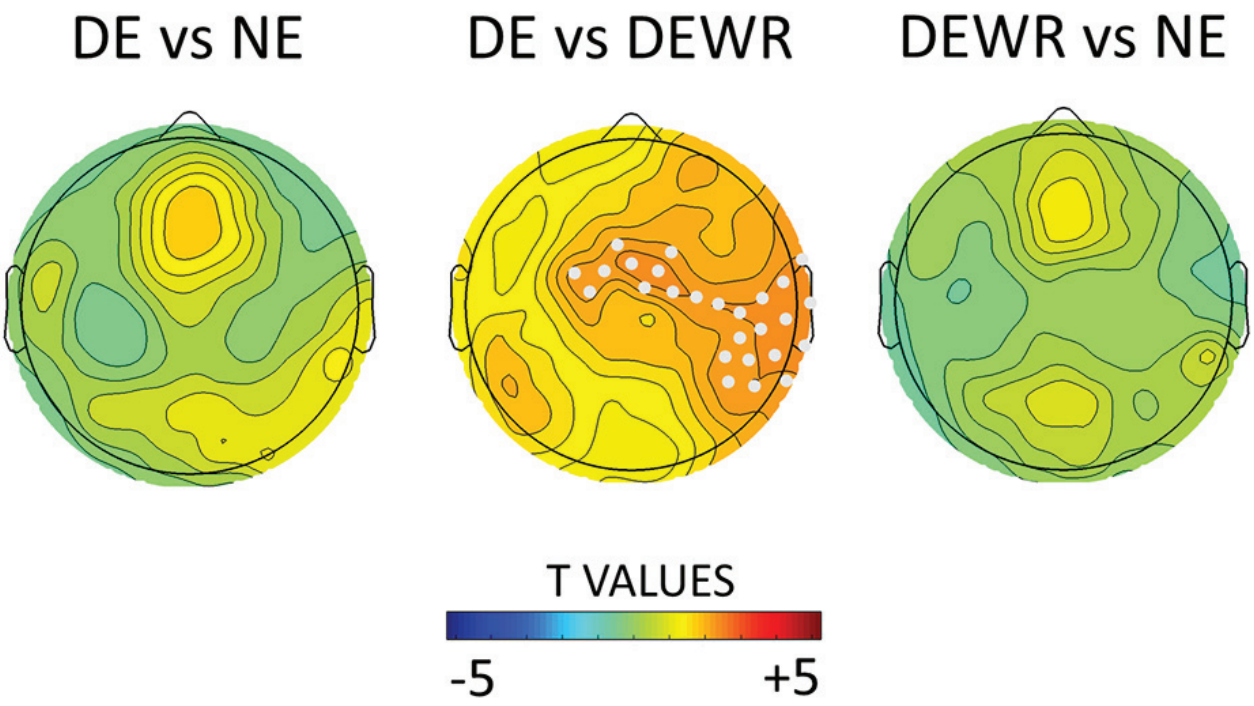

JNeurosci Accepted Manuscript

DREAM EXPERIENCE VS NO EXPERIENCE

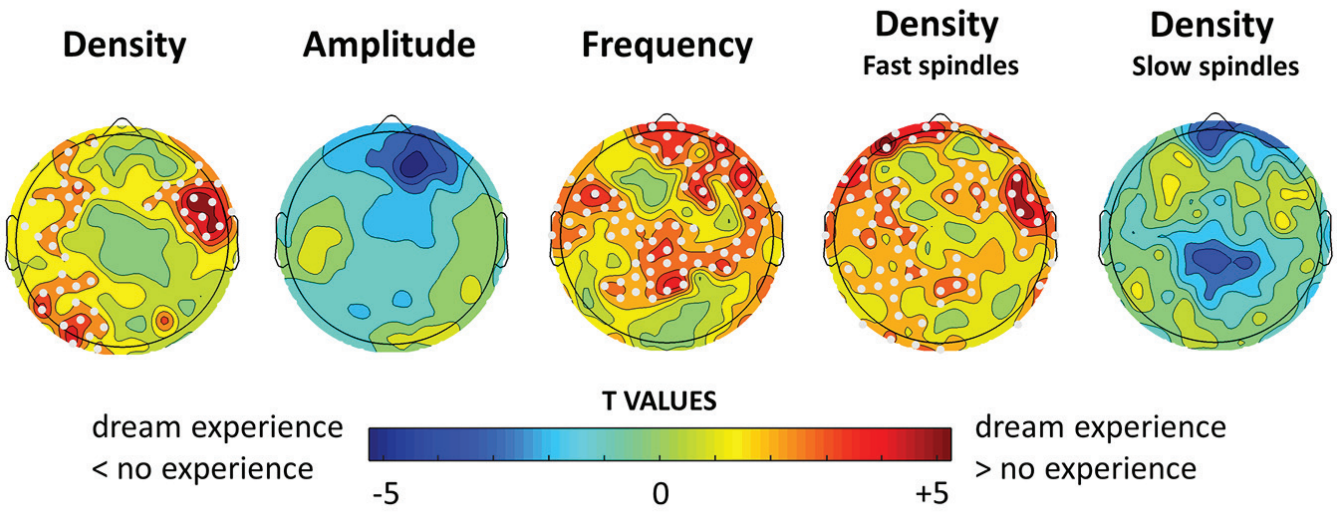

DREAM EXPERIENCE W/O RECALL OF CONTENT VS NO EXPERIENCE